

# LONG-RUN AVAILABILITY OF A PRIORITY SYSTEM: A NUMERICAL APPROACH

EDMOND J. VANDERPERRE AND STANISLAV S. MAKHANOV

*Received 29 June 2004*

We consider a two-unit cold standby system attended by two repairmen and subjected to a priority rule. In order to describe the random behavior of the twin system, we employ a stochastic process endowed with state probability functions satisfying coupled Hokstad-type differential equations. An explicit evaluation of the exact solution is in general quite intricate. Therefore, we propose a numerical solution of the equations. Finally, particular but important repair time distributions are involved to analyze the long-run availability of the **T**-system. Numerical results are illustrated by adequate computer-plotted graphs.

## 1. Introduction

Standby provides a powerful tool to enhance the reliability, availability, quality, and safety of operational plants, see, for example, [3, 7, 14]. However, in practice, standby systems are often subjected to an appropriate priority rule. For instance, the *external* power supply station of a technical plant has usually overall priority in operation with regard to an *internal* (local) power generator kept in cold or warm standby [3]. The local generator is only deployed if the external power station is down.

Cold or warm standby systems subjected to a priority rule and attended by a repair facility have received considerable attention in the current literature, see, for example, [1, 2, 4, 5, 8, 9, 10, 11, 12, 13, 16, 17, 18, 19, 20, 21].

As a variant, we consider a twin system composed of a priority unit (the **p**-unit) and a nonpriority unit (the **n**-unit) kept in *cold* standby. The **p**-unit has *overall* (break-in) priority in operation with regard to the **n**-unit, that is, the **n**-unit is only used when the **p**-unit is down. In order to avoid undesirable delays in repairing failed units, we suppose that the entire system (henceforth called the **T**-system) is attended by *two* different repairmen. The **T**-system satisfies the usual conditions, that is, independent identically distributed random variables, instantaneous and perfect switch [3], and perfect repair [6]. Each repairman has his own particular task. Repairman  $\mathcal{N}$  is skilled in repairing the **n**-unit, whereas repairman  $\mathcal{P}$  is an expert in repairing the **p**-unit. Both repairmen are jointly busy, if and only if, both units (**p**-unit and **n**-unit) are down. In any other case, at least one repairman is idle.

In order to describe the *random* behavior of the **T**-system, we employ a stochastic process endowed with transition probability functions satisfying steady-state Hokstad-type differential equations. Unfortunately, the *exact* solution procedure is quite intricate (see, [21, page 359] and Remark 4.1). Therefore, we propose a *numerical* solution of the equations.

Finally, current repair time distributions (such as the Weibull-Gnedenko distribution) are involved to compute the long-run availability of the **T**-system. The results are illustrated by adequate computer-plotted graphs.

## 2. Formulation

Consider a **T**-system satisfying the usual conditions. The **p**-unit has a constant failure rate [15]  $\lambda > 0$  and a general repair time distribution  $R(\cdot), R(0) = 0$ , with mean  $\rho$ . The *operative* **n**-unit has a constant failure rate  $\lambda_s > 0$ , but a *zero* failure rate in standby (the so-called cold standby state) and a general repair time distribution  $R_S(\cdot), R_S(0) = 0$ , with mean  $\rho_s$ . In order to describe the random behavior of the **T**-system, we introduce a stochastic process  $\{N_t, t \geq 0\}$  with arbitrary discrete state space  $\{A, B, C, D\} \subset [0, \infty)$ , characterized by the following mutually exclusive events:

- (i)  $\{N_t = A\}$ : “the **p**-unit is operative and the **n**-unit is in cold standby at time  $t$ ,”
- (ii)  $\{N_t = B\}$ : “the **n**-unit is operative and the **p**-unit is under repair at time  $t$ ,”
- (iii)  $\{N_t = C\}$ : “the **p**-unit is operative and the **n**-unit is under repair at time  $t$ ,”
- (iv)  $\{N_t = D\}$ : “both units are simultaneously down at time  $t$ .”

State  $D$  is called the system-down state.

Figures 2.1, 2.2, 2.3, and 2.4 display a functional block diagram of the **T**-system operating in states  $A, B, C$ , and  $D$ .

Observe that the process  $\{N_t, t \geq 0\}$  is non-Markovian. A Markov characterization of the process is piecewise and conditionally defined by:

- (i)  $\{N_t\}$ , if  $N_t = A$  (i.e., if the event  $\{N_t = A\}$  occurs),
- (ii)  $\{(N_t, X_t)\}$ , if  $N_t = B$ , where  $X_t$  denotes the *remaining* repair time of the **p**-unit under progressive repair at time  $t$ ,
- (iii)  $\{(N_t, Y_t)\}$ , if  $N_t = C$ , where  $Y_t$  denotes the *remaining* repair time of the **n**-unit under progressive repair at time  $t$ ,
- (iv)  $\{(N_t, X_t, Y_t)\}$ , if  $N_t = D$ .

The state space of the underlying piecewise linear (vector) Markov process is given by

$$A \cup \{(B, x); x \geq 0\} \cup \{(C, y); y \geq 0\} \cup \{(D, x, y); x \geq 0; y \geq 0\}. \quad (2.1)$$

Next, we consider the **T**-system in stationary state (the so-called *ergodic* state) with *invariant* measure  $\{p_K; K = A, B, C, D\}$ ,  $\sum_K p_K = 1$ , where

$$p_K := \lim_{t \rightarrow \infty} \mathbf{P}\{N_t = K | N_0 = A\}. \quad (2.2)$$

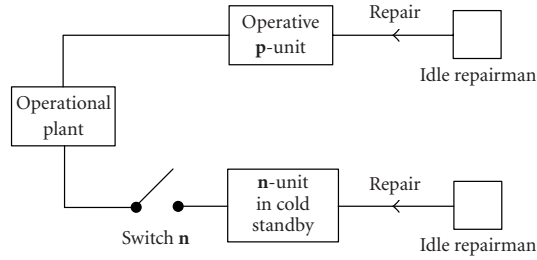


Figure 2.1. Functional block diagram of the T-system operating in state A.

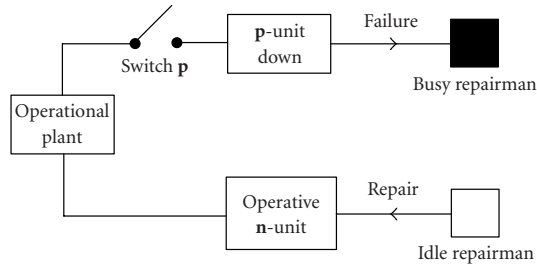


Figure 2.2. Functional block diagram of the T-system operating in state B.

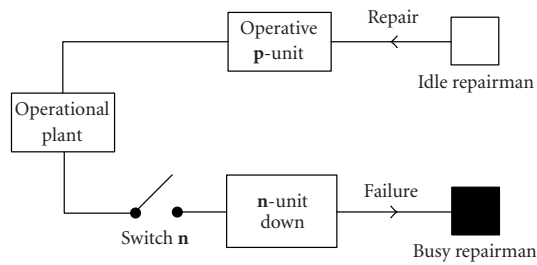


Figure 2.3. Functional block diagram of the T-system operating in state C.

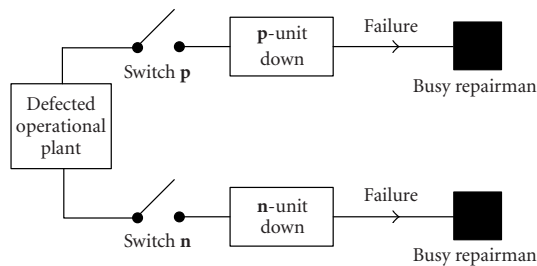


Figure 2.4. Functional block diagram of the T-system in state D.

It can be demonstrated that the invariant measure exists for arbitrary  $R$  and  $R_S$  with finite mean. However, in order to keep the analysis as simple as possible, we henceforth assume that  $R$  and  $R_S$  have *bounded* densities on  $[0, \infty)$ , denoted by  $r$  and  $r_s$ . Finally, we introduce the measures

$$\begin{aligned} p_B(x)dx &:= \lim_{t \rightarrow \infty} \mathbf{P}\{N_t = B, X_t \in (x, x + dx) | N_0 = A\}, \\ p_C(y)dy &:= \lim_{t \rightarrow \infty} \mathbf{P}\{N_t = C, Y_t \in (y, y + dy) | N_0 = A\}, \\ p_D(x, y)dx dy &:= \lim_{t \rightarrow \infty} \mathbf{P}\{N_t = D, X_t \in (x, x + dx), Y_t \in (y, y + dy) | N_0 = A\}. \end{aligned} \quad (2.3)$$

Note that, for instance,  $p_D = \int_0^\infty \int_0^\infty p_D(x, y)dx dy$ .

### 3. Long-run availability

We recall that the  $\mathbf{T}$ -system is only available (functioning) in states  $A$ ,  $B$ , and  $C$ . Therefore, the *long-run* availability of the operational plant, denoted by  $\mathcal{A}$ , is given by  $\mathcal{A} = 1 - p_D$ . Invoking the substitutions  $p_B(\cdot) = p_A \varphi_B(\cdot)$ ,  $p_C(\cdot) = p_A \varphi_C(\cdot)$ ,  $p_D(\cdot, \cdot) = p_A \varphi_D(\cdot, \cdot)$  and the law  $\sum_K p_K = 1$  entails that  $p_A = 1/(1 + \Phi_B + \Phi_C + \Phi_D)$ , where  $\Phi_B := \int_0^\infty \varphi_B(x)dx$ ,  $\Phi_C := \int_0^\infty \varphi_C(y)dy$  and  $\Phi_D := \int_0^\infty \int_0^\infty \varphi_D(x, y)dx dy$ . Hence,

$$\mathcal{A} = \frac{1 + \Phi_B + \Phi_C}{1 + \Phi_B + \Phi_C + \Phi_D}. \quad (3.1)$$

### 4. Differential equations

In order to determine the  $\varphi$ -functions, we first construct a system of coupled steady state-type differential equations based on a time-independent version of Hokstad's supplementary variable technique (see, e.g., [22, page 526] for further details). For  $x > 0$ ,  $y > 0$ , we obtain

$$\lambda = \varphi_B(0) + \varphi_C(0), \quad (4.1)$$

$$\left(\lambda_s - \frac{d}{dx}\right) \varphi_B(x) = \varphi_D(x, 0) + \lambda r(x), \quad (4.2)$$

$$\left(\lambda - \frac{d}{dy}\right) \varphi_C(y) = \varphi_D(0, y), \quad (4.3)$$

$$\left(-\frac{\partial}{\partial x} - \frac{\partial}{\partial y}\right) \varphi_D(x, y) = \lambda_s \varphi_B(x) r_s(y) + \lambda \varphi_C(y) r(x). \quad (4.4)$$

*Remark 4.1.* A particular but important family  $\mathcal{F}$  of current repair time distributions with nonrational characteristic functions, such as the Weibull-Gnedenko and Lognormal distributions, are fairly suitable to model repair times. Unfortunately, if both  $R$  and  $R_S$  belong to  $\mathcal{F}$ , an explicit evaluation of the *exact* solution of (4.1), (4.2), (4.3), and (4.4) in terms of *finite* linear combinations of known algebraic and/or transcendental functions is as good as excluded (see [21, page 361] for further details). Therefore, we propose a *numerical* solution of the equations.

### 5. Numerical scheme

In order to construct an appropriate numerical procedure, we first remark that the  $\varphi$ -functions are vanishing at infinity *irrespective* of the asymptotic behavior of the repair time density functions! Therefore, a numerical procedure to solve the equations in the region  $(0, \infty) \times (0, \infty)$  may be converted into a numerical solution procedure in the *truncated* region  $(0, L) \times (0, L)$ , for some  $L > 0$ , with prescribed boundary conditions  $\varphi_B(L) = \varphi_C(L) = \varphi_D(L, \cdot) = \varphi_D(\cdot, L) = 0$ . Let  $\varphi_{B,i} := \varphi_B(x_i)$ ,  $\varphi_{C,j} := \varphi_C(y_j)$ ,  $\varphi_{D,i,j} := \varphi_D(x_i, y_j)$ , where  $x_i := i\Delta$ ,  $y_j := j\Delta$ ,  $i = 0, \dots, N + 1$ ;  $j = 0, \dots, N + 1$ ;  $\Delta := L/N$ . We propose the following numerical scheme. Let  $k$  be the iteration number. Given  $\varphi_{D,i,N+1}^{k+1} = 0$ ,  $\varphi_{D,N+1,j}^{k+1} = 0$ ,  $\varphi_{B,N+1}^{k+1} = 0$ ,  $\varphi_{C,N+1}^{k+1} = 0$ , and the values of  $\varphi_{B,i}^k$  and  $\varphi_{C,j}^k$ , we compute  $\varphi_{D,i,j}^{k+1}$  by means of the two-point first-order approximation of (4.4), namely,

$$\varphi_{D,i,j}^{k+1} = \frac{1}{2}(\varphi_{D,i,j+1}^{k+1} + \varphi_{D,i+1,j}^{k+1}) + \frac{\Delta}{2}(\lambda_s \varphi_{B,i}^k r_{s,j} + \lambda \varphi_{C,j}^k r_i), \tag{5.1}$$

$i = N, N - 1, \dots, 0$  and  $j = N, N - 1, \dots, 0$ .

Next, we calculate  $\varphi_{B,i}^{k+1}$  and  $\varphi_{C,j}^{k+1}$  by means of the first-order approximations of (4.2) and (4.3) given by

$$\begin{aligned} \varphi_{B,i}^{k+1} &= \frac{1}{\gamma_B} \left( \frac{\varphi_{B,i+1}^{k+1}}{\Delta} + \varphi_{D,i,0}^{k+1} + \lambda r_i \right), \\ \varphi_{C,j}^{k+1} &= \frac{1}{\gamma_C} \left( \frac{\varphi_{C,j+1}^{k+1}}{\Delta} + \varphi_{D,0,j}^{k+1} \right), \end{aligned} \tag{5.2}$$

where  $\gamma_B := \lambda_s + 1/\Delta$  and  $\gamma_C := \lambda + 1/\Delta$ . Finally, in order to satisfy (4.1) we use the normalizing procedure

$$\begin{aligned} \varphi_{C,j}^{k+1, \text{new}} &= \lambda \frac{\varphi_{C,j}^{k+1}}{\varphi_{C,0}^{k+1} + \varphi_{B,0}^{k+1}}, \\ \varphi_{B,i}^{k+1, \text{new}} &= \lambda \frac{\varphi_{B,i}^{k+1}}{\varphi_{C,0}^{k+1} + \varphi_{B,0}^{k+1}}. \end{aligned} \tag{5.3}$$

*Remarks 5.1.* Let  $\varphi_\Delta$  denote a numerical solution obtained with the space-step  $\Delta$ . The relevant numerical error is then evaluated on a nested grid by  $\varepsilon := |\varphi_\Delta - \varphi_{\Delta/2}|$ . However, such an estimate is only accurate if  $L$  is large enough. Roughly speaking, if  $\max(r(x), r_s(x))$  at  $x = L$  is small, then (most likely) this particular  $L$  is appropriate. However, such a “brutal force” approach may require a large number of grid points and is therefore rarely applicable. We illustrate the phenomenon by comparing the exact and the numerical solution in the most simple case, that is, let  $R(x) = 1 - e^{-x}$ ,  $R_S(y) = 1 - e^{-y}$ . Then,  $\varphi_D(x, y) = l_D e^{-(x+y)}$ ,  $\varphi_C(y) = l_C e^{-y}$ ,  $\varphi_B(x) = l_B e^{-x}$ , where  $l_D := \lambda_s(\lambda + 1)\lambda/(\lambda_s + \lambda + 2)$ ,  $l_C := \lambda_s\lambda/(\lambda_s + \lambda + 2)$ ,  $l_B := \lambda(\lambda + 2)/(\lambda_s + \lambda + 2)$ .

Figure 5.1 shows the numerical error

$$\varepsilon_M := \max \{ |\varphi_D^{\text{exact}} - \varphi_D|, |\varphi_C^{\text{exact}} - \varphi_C|, |\varphi_B^{\text{exact}} - \varphi_B| \} \tag{5.4}$$

versus the grid size for various  $L$ .

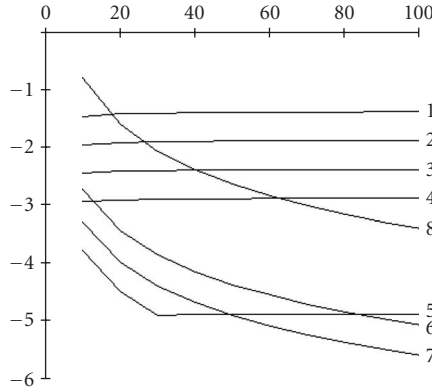


Figure 5.1. The horizontal axis denotes the logarithm of the numerical error, the vertical axis denotes the number of the grid points, (1)  $L = 0.4$ ; (2)  $L = 1.0$ ; (3)  $L = 1.5$ ; (4)  $L = 2$ ; (5)  $L = 4$ ; (6)  $L = 6$ ; (7)  $L = 10$ ; (8)  $L = 50$ .

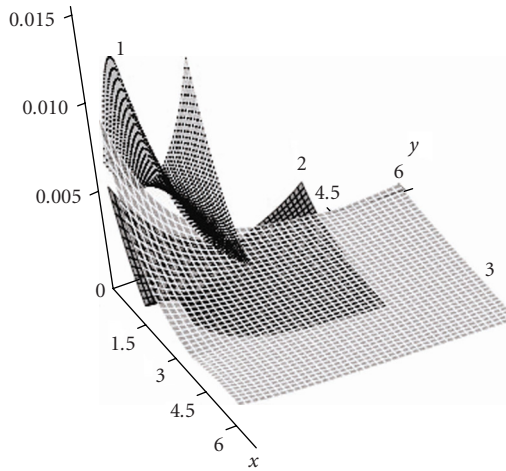


Figure 5.2. Spatial distribution of  $\varepsilon_D$ , (1)  $L = 1.5$ ; (2)  $L = 3$ ; (3)  $L = 6$ .

Observe that, if  $L$  is not large enough,  $\varepsilon_M$  does not decrease as  $\Delta$  decreases (see Figure 5.1). On the other hand, too large  $L$  (consequently, too large  $\Delta$ ) lead to large numerical errors. For instance, the error with  $L = 30$  is larger than  $2.5 \cdot 10^{-2}$  for any  $N \in [20, 100]$ , whereas the error with  $L = 4$  is less than  $2.5 \cdot 10^{-2}$ . There could be multiple options too. For instance, an error less than  $2.5 \cdot 10^{-2}$  is achieved either with  $L = 4$ ,  $N = 15$ , or  $L = 6$ ,  $N = 22$ , or  $L = 10$ ,  $N = 38$ .

Figure 5.2 shows a two-dimensional spatial distribution of the error  $\varepsilon_D := |\varphi_D^{\text{exact}} - \varphi_D|$  for various  $L$ . Clearly,  $\varepsilon_D$  could be increasing near the origin as  $L$  increases. However, the error decreases for large  $x$  and  $y$ .

**6. Trial-and-error procedure**

The complicated behavior of the numerical error requires an adaptive choice of  $\Delta$  and  $L$ . Therefore, we introduce the subordinate errors  $\varepsilon_1 := |\varphi_{\Delta,L} - \varphi_{\Delta,L/2}|$  and  $\varepsilon_2 := |\varphi_{\Delta,L} - \varphi_{\Delta/2,L}|$ , where  $\varepsilon_1$  characterizes the numerical error caused by truncation of the infinite region and  $\varepsilon_2$  the numerical error related to the first-order approximants. In order to find the optimal pair  $(L, \Delta)$ , we first specify the required accuracy  $\varepsilon$ . Next, we propose the following trial-and-error procedure: *we vary  $L$  until  $\varepsilon_1 < \varepsilon$  and then  $\Delta$  until  $\varepsilon_2 < \varepsilon$* . Finally, we introduce the following.

**7. Application. The Weibull-Gnedenko distribution**

We consider the particular but important case of Weibull-Gnedenko repair time distributions, that is, let  $R(x) = 1 - e^{-x^{\beta_1}}$ ,  $R_S(y) = 1 - e^{-y^{\beta_2}}$ . Obviously, the optimal pair  $(L, \Delta)$  depends on  $\lambda, \lambda_s, \beta_1$ , and  $\beta_2$ . We demonstrate the trial-and-error procedure applied to the particular case  $\lambda = 1, \lambda_s = 0.1, \beta_1 = 2, \beta_2 = 3$ . However, no restrictions are imposed on the analysis of  $\mathcal{A}$  for arbitrary values of  $\lambda, \lambda_s, \beta_1$  and  $\beta_2$ . Let  $\varepsilon = 10^{-3}$ .

First, we vary  $L$ , as shown in Table 7.1, until  $\varepsilon_1 < \varepsilon$ . Next, we vary  $\Delta$ , as shown in Table 7.2, until  $\varepsilon_2 < \varepsilon$ . A spatial distribution of  $\varepsilon_1$  and  $\varepsilon_2$  is depicted in Figures 7.1 and 7.2.

Table 7.1. The  $L$  trials.

$L$	$N$	$\Delta$	$\varepsilon_1$
3	40	3/40	$1.9 \cdot 10^{-2}$
6	80	3/40	$7.4 \cdot 10^{-4}$

Table 7.2. The  $\Delta$  trials.

$L$	$N$	$\Delta$	$\varepsilon_2$
6	80	3/40	$6.8 \cdot 10^{-3}$
6	160	3/80	$3.3 \cdot 10^{-3}$
6	320	3/160	$9.2 \cdot 10^{-4}$

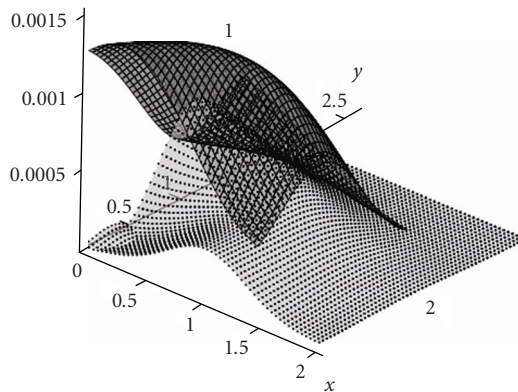


Figure 7.1. Spatial distribution of  $\varepsilon_1$ , (1)  $L = 3$ ; (2)  $L = 6$ .

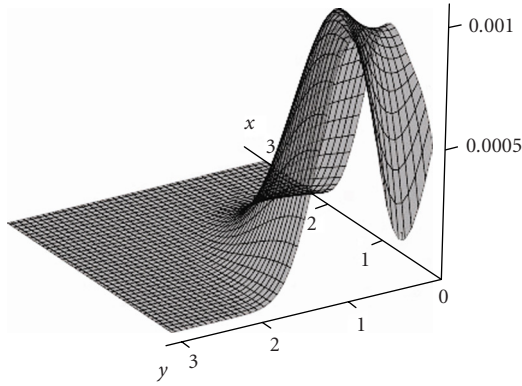


Figure 7.2. Spatial distribution of  $\varepsilon_2$  for  $N = 320$ .

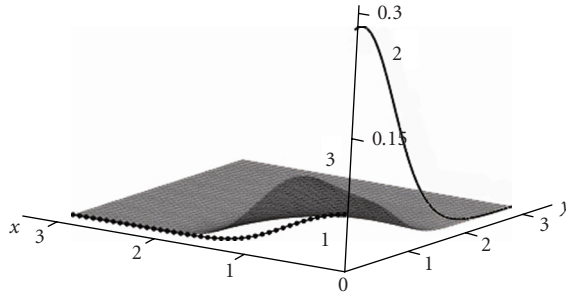


Figure 7.3. Numerically generated: (1)  $p_B(x)/1.5$ , (2)  $p_C(x)$ , (3)  $p_D(x, y)$ ,  $\lambda_s = 0.3$   $\lambda = 1.0$ . Note that  $p_B$  is divided by 1.5 due to scaling.

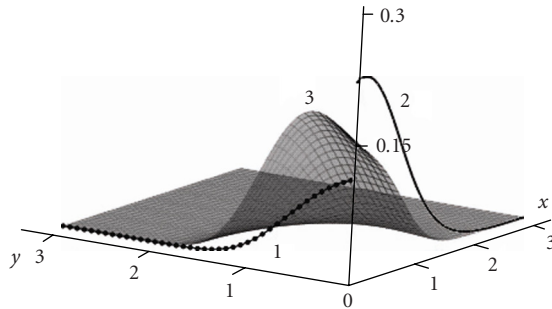


Figure 7.4. Numerically generated: (1)  $p_B(x)/1.5$ , (2)  $p_C(x)$ , (3)  $p_D(x, y)$ ,  $\lambda_s = 0.7$   $\lambda = 1.0$ . Note that  $p_B$  is divided by 1.5 due to scaling.

Figure 7.3 displays  $p_B(\cdot)$ ,  $p_C(\cdot)$ , and  $p_D(\cdot, \cdot)$  for  $\lambda = 1$ ,  $\lambda_s = 0.3$  and Figure 7.4 for  $\lambda = 1$ ,  $\lambda_s = 0.5$ . Figure 7.5 shows  $p_D(x, y)$  for various  $\lambda_s$ . Let  $\mathcal{A}_{\beta_1, \beta_2}(\lambda, \lambda_s)$  denote the long-run availability as a function of  $\lambda$  and  $\lambda_s$ .



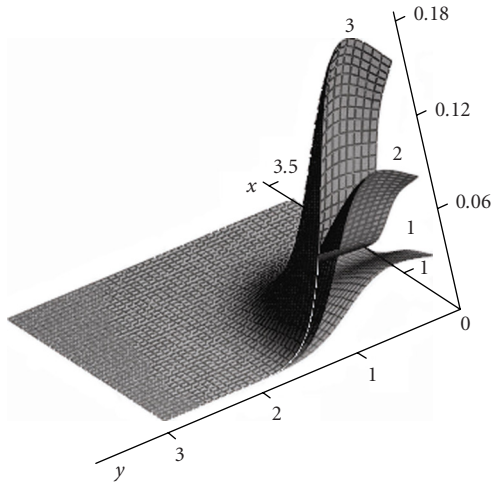


Figure 7.5. Numerically generated  $p_D(x, y)$ ,  $\lambda = 1.0$ , (1)  $\lambda_s = 0.1$ , (2)  $\lambda_s = 0.3$ , (3)  $\lambda_s = 0.7$ .

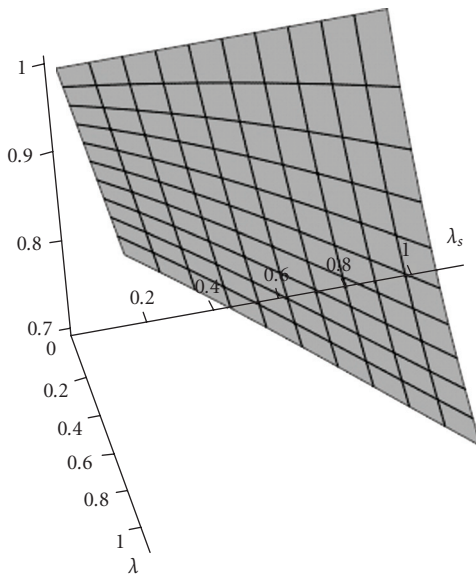


Figure 7.6. Numerically generated long-run availability.

Figure 7.6 shows that the long-run availability exhibits a nonlinear behavior for sufficiently large  $\lambda$  and  $\lambda_s$  (see also Table 7.3). Finally, Figure 7.7 displays the deviations  $d_1 := |\mathcal{A}_{2,2} - \mathcal{A}_{2,4}|$ ,  $d_2 := |\mathcal{A}_{2,2} - \mathcal{A}_{4,2}|$ ,  $d_3 := |\mathcal{A}_{2,2} - \mathcal{A}_{4,4}|$ . The plot reveals that  $\mathcal{A}$  is fairly insensitive for  $\beta$ -variations.

Table 7.3. Long-run availability  $\mathcal{A}_{2,2}(\lambda, \lambda_s)$ .

$\lambda/\lambda_s$	0.1	0.2	0.3	0.4	0.5	0.6	0.7	0.8	0.9	1.0
0.1	0.9950	0.9895	0.9837	0.9775	0.9709	0.9640	0.9566	0.9489	0.9408	0.9324
0.2	0.9908	0.9811	0.9706	0.9596	0.9480	0.9358	0.9231	0.9098	0.8962	0.8821
0.3	0.9874	0.9740	0.9599	0.9450	0.9295	0.9133	0.8965	0.8792	0.8615	0.8434
0.4	0.9845	0.9681	0.9509	0.9330	0.9143	0.8949	0.8750	0.8546	0.8338	0.8128
0.5	0.9820	0.9631	0.9434	0.9229	0.9016	0.8797	0.8573	0.8345	0.8114	0.7882
0.6	0.9798	0.9588	0.9369	0.9143	0.8909	0.8670	0.8426	0.8179	0.7930	0.7680
0.7	0.9779	0.9550	0.9313	0.9069	0.8818	0.8562	0.8301	0.8039	0.7775	0.7512
0.8	0.9762	0.9517	0.9265	0.9005	0.8740	0.8469	0.8195	0.7920	0.7644	0.7370
0.9	0.9748	0.9488	0.9222	0.8949	0.8671	0.8389	0.8103	0.7817	0.7532	0.7249
1.0	0.9734	0.9462	0.9184	0.8900	0.8611	0.8318	0.8024	0.7729	0.7435	0.7145

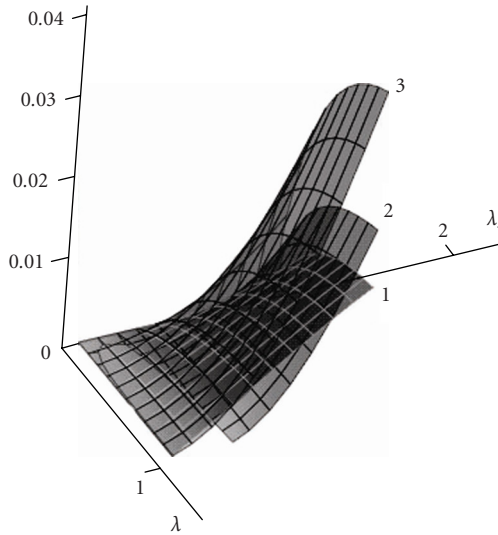


Figure 7.7. Spatial deviations  $d_i, i = 1, 2, 3$ .

### 8. Conclusion

An effective statistical analysis of the T-system requires the solution of coupled Hokstad-type differential equations. Our numerical solution procedure, endowed with a simple and robust algorithm, allows to compute and to analyze the long-run availability for a general class of current repair time distributions with tangible engineering applications.

### References

[1] J. R. Arora, *Reliability of a two-unit priority standby redundant system with finite repair capability*, IEEE Trans. Reliab. **R-25** (1976), 205–207.

- [2] ———, *Reliability of several standby priority redundant systems*, IEEE Trans. Reliab. **R-30** (1981), 123–132.
- [3] A. Birolini, *Quality and Reliability of Technical Systems*, Springer-Verlag, Berlin, 1994.
- [4] J. A. Buzacott, *Availability of priority redundant systems*, IEEE Trans. Reliab. **R-20** (1971), 60–63.
- [5] B. B. Fawzi and A. G. Hawkes, *Availability of a series system with replacement and repair*, J. Appl. Probab. **27** (1990), no. 4, 873–887.
- [6] I. B. Gertsbakh, *Statistical Reliability Theory, Probability: Pure and Applied*, vol. 4, Marcel Dekker, New York, 1989.
- [7] B. Gnedenko and I. A. Ushakov, *Probabilistic Reliability Engineering*, John Wiley & Sons, New York, 1995.
- [8] L. R. Goel and S. K. Singh, *Cost analysis of a two-unit priority standby system with imperfect switch, intermittent repair and arbitrary distributions*, IEEE Trans. Reliab. **R-35** (1986), 585–586.
- [9] R. Gupta and L. R. Goel, *Profit analysis of a two-unit priority standby system with administrative delay in repair*, Internat. J. Systems Sci. **20** (1998), 1703–1712.
- [10] W. Li and D. H. Shi, *Reliability analysis of a two-dissimilar-unit parallel redundant system with preemptive priority rule*, Microelectron. Reliab. **33** (1993), no. 10, 1447–1453.
- [11] H. Mine, *Repair priority effect on the availability of a two-unit system*, IEEE Trans. Reliab. **R-28** (1979), 325–326.
- [12] T. Nakagawa and S. Osaki, *Stochastic behaviour of a two-unit priority standby redundant system with repair*, Microelectron. Reliab. **14** (1975), no. 3, 309–313.
- [13] S. Osaki, *Reliability analysis of a two-unit standby redundant system with priority*, Can. Oper. Res. Soc. J. **8** (1970), 60–62.
- [14] H. Pham, *Recent Advances in Reliability and Quality Engineering*, World Scientific Publishing, Singapore, 2001.
- [15] M. Shaked and J. G. Shanthikumar, *Reliability and maintainability*, Stochastic Models (D. P. Heyman and M. J. Sobel, eds.), Handbooks Oper. Res. Management Sci., vol. 2, North-Holland, Amsterdam, 1990, pp. 653–713.
- [16] D.-H. Shi and L. Liu, *Availability analysis of a two-unit series system with a priority shut-off rule*, Naval Res. Logist. **43** (1996), no. 7, 1009–1024.
- [17] R. Subramanian and N. Ravichandran, *Probabilistic analysis of a two-unit standby redundant system with finite repair capacity*, Opsearch **17** (1980), no. 2-3, 71–80.
- [18] ———, *Analysis of a two unit warm standby system*, Opsearch **21** (1984), 23–29.
- [19] K. Val'des Kastro, *Optimal policies in a priority standby model*, Vestnik Moskov. Univ. Ser. I Mat. Mekh. **41** (1986), no. 4, 10–15.
- [20] E. J. Vanderperre, *Reliability analysis of a two-unit cold standby redundant system subject to a priority rule*, Cahiers Centre Études Rech. Opér. **31** (1989), no. 1-2, 159–166.
- [21] ———, *Long-run availability of a two-unit standby system subjected to a priority rule*, Bull. Belg. Math. Soc. Simon Stevin **7** (2000), no. 3, 355–364.
- [22] E. J. Vanderperre, S. S. Makhanov, and S. Suchatvejapoom, *Long-run availability of a repairable parallel system*, Microelectron. Reliab. **37** (1997), no. 3, 525–527.

Edmond J. Vanderperre: Department of Quantitative Management, University of South Africa,  
P.O. Box 392, Pretoria 0003, South Africa  
*E-mail address:* edmondvanderperre@hotmail.com

Stanislav S. Makhanov: Faculty of Information Technology, Sirindhorn International Institute of  
Technology, Thammasat University, P.O. Box 22, Patumthani 12121, Thailand  
*E-mail address:* makhanov@siit.tu.ac.th

## Special Issue on Decision Support for Intermodal Transport

### Call for Papers

Intermodal transport refers to the movement of goods in a single loading unit which uses successive various modes of transport (road, rail, water) without handling the goods during mode transfers. Intermodal transport has become an important policy issue, mainly because it is considered to be one of the means to lower the congestion caused by single-mode road transport and to be more environmentally friendly than the single-mode road transport. Both considerations have been followed by an increase in attention toward intermodal freight transportation research.

Various intermodal freight transport decision problems are in demand of mathematical models of supporting them. As the intermodal transport system is more complex than a single-mode system, this fact offers interesting and challenging opportunities to modelers in applied mathematics. This special issue aims to fill in some gaps in the research agenda of decision-making in intermodal transport.

The mathematical models may be of the optimization type or of the evaluation type to gain an insight in intermodal operations. The mathematical models aim to support decisions on the strategic, tactical, and operational levels. The decision-makers belong to the various players in the intermodal transport world, namely, drayage operators, terminal operators, network operators, or intermodal operators.

Topics of relevance to this type of decision-making both in time horizon as in terms of operators are:

- Intermodal terminal design
- Infrastructure network configuration
- Location of terminals
- Cooperation between drayage companies
- Allocation of shippers/receivers to a terminal
- Pricing strategies
- Capacity levels of equipment and labour
- Operational routines and lay-out structure
- Redistribution of load units, railcars, barges, and so forth
- Scheduling of trips or jobs
- Allocation of capacity to jobs
- Loading orders
- Selection of routing and service

Before submission authors should carefully read over the journal's Author Guidelines, which are located at <http://www.hindawi.com/journals/jamds/guidelines.html>. Prospective authors should submit an electronic copy of their complete manuscript through the journal Manuscript Tracking System at <http://mts.hindawi.com/>, according to the following timetable:

Manuscript Due	June 1, 2009
First Round of Reviews	September 1, 2009
Publication Date	December 1, 2009

### Lead Guest Editor

**Gerrit K. Janssens**, Transportation Research Institute (IMOB), Hasselt University, Agoralaan, Building D, 3590 Diepenbeek (Hasselt), Belgium; [Gerrit.Janssens@uhasselt.be](mailto:Gerrit.Janssens@uhasselt.be)

### Guest Editor

**Cathy Macharis**, Department of Mathematics, Operational Research, Statistics and Information for Systems (MOSI), Transport and Logistics Research Group, Management School, Vrije Universiteit Brussel, Pleinlaan 2, 1050 Brussel, Belgium; [Cathy.Macharis@vub.ac.be](mailto:Cathy.Macharis@vub.ac.be)